

Available online at: <http://ajeet.ft.unand.ac.id/>

Andalas Journal of Electrical and Electronic Engineering Technology

ISSN 2777-0079



Research Article

DC-DC Buck and Boost Converter Design for Energy Control in Hybrid PV Systems

Zaini, Wisnu Joko Wulung

Electrical Engineering Department, Faculty of Engineering, Universitas Andalas, Padang, Indonesia 25163

ARTICLE INFORMATION

Received: June 26, 2023
 Revised: November 26, 2023
 Accepted: November 28, 2023
 Available online: November 30, 2023

KEYWORDS

DC-DC Converter, PID, Load Demand, Hybrid PV, Simulink, Matlab

CORRESPONDENCE

Phone: +62-81266224644
 E-mail: zzaini21@gmail.com

A B S T R A C T

The intermittent nature of photovoltaic (PV) power generation due to weather conditions and time of day can affect the ability of PV systems to satisfy load demand. An effective PV system must store excess electrical energy when generation exceeds demand and discharge stored energy when demand is greater than generation. This study utilizes MATLAB simulations to design and evaluate DC-DC converter circuits for battery charging and discharging in PV systems. For charging, a buck converter with a fixed 45 V source is able to reduce voltage to a range of 33.99 V to 1.46 V by decreasing the duty cycle. For discharging, a boost converter with a fixed 12.8 V source can increase voltage to 16.90 V–33.49 V by raising the duty cycle. Furthermore, under equal comparison, the open-loop buck converter operating at a 35% duty cycle demonstrates worse overshoot of 14.36% versus 0.24% for the closed-loop PID controlled buck converter. Similarly, the open-loop boost converter at 70% duty cycle exhibits slightly higher overshoot of 0.47% compared to negligible overshoot for the closed-loop PID controlled boost converter.

INTRODUCTION

The global energy crisis [1] and climate change [2] have motivated many countries to gradually transition from non-renewable energy sources to renewable alternatives [3], [4]. Solar photovoltaics (PV) in particular offer the advantages of an abundant renewable resource [5] and zero emissions during operation [6]. However, solar PV output intermittency poses challenges, as the intensity of solar irradiation fluctuates with weather conditions and time of day [7], [8], preventing continuous absorption by PV panels. Overcoming solar intermittency is crucial for enabling higher PV penetrations while maintaining grid reliability.

Solar photovoltaic (PV) intermittency poses reliability challenges for meeting residential load demand in Indonesia, as peak electricity consumption times are often inverse to peak production times [9]. Appropriate PV system design is therefore critical, potentially incorporating DC-DC converters for battery energy storage and discharge [10]–[12]. Storage enables supply during high demand periods when generation is insufficient, while charging during low demand allows excess PV generation to be captured.

This work focuses on a 600 Wp PV system capable of meeting electricity needs for middle to lower income Indonesian households. The system size dictates key DC-DC converter

parameters for the buck and boost converter designs presented. The buck converter steps down PV voltage for battery charging, while the boost enables higher voltage discharging to meet load demand. Maintaining output current and voltage set points enables effective PV energy time-shifting.

Prior relevant works have explored similar DC-DC converter applications but differ in aspects like MPPT utilization, converter topologies, and load supply configurations [13]–[15]. By detailing basic buck and boost converter design for PV energy storage and discharge, this research provides fundamental insights for improved PV reliability via DC-DC conversion.

The key objectives were to 1) highlight the motivation around PV intermittency and residential demand mismatch, 2) summarize the core technical approach of using DC-DC converters for battery charging/discharging to time-shift solar energy, and 3) differentiate the focus of this work compared to prior arts.

METHOD

In this study, the design of DC-DC Buck and Boost Converter for storing and discharging electrical energy using a battery in a PV Hybrid system was carried out using Simulink MATLAB software. This simulation modeling is important to do in the initial stages of converter circuit design in order to minimize

various system failures that might occur in the future, if the real form of the converter design has been made in the form of a PCB circuit.

Then, based on the system block diagram in Figure 1 below, it can be seen that PV as a source of electricity has two options to continue the dc energy it produces, namely to charge the battery with a dc-dc buck converter component, or PV is used directly to supply ac loads with inverter component. In addition, not only PV but also a battery that has been fully charged by PV can also be used as a power source to supply AC loads by first passing it to the DC-DC boost converter and inverter components as seen in Figure 1.

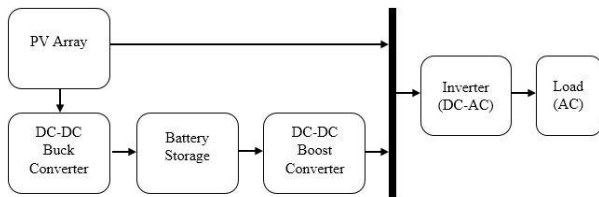


Figure 1. DC-DC Converter Block Diagram in Hybrid PV Systems with PV and Batteries as Power Sources

PV Array

The solar panel module used in this study is a monocrystalline SOL-M12150W type with a module output power of 150 Wp [16]. Furthermore, in the PV system, four units of solar panel modules are used in series-parallel so that the Voc and Isc values are approximately 44.2 V and 17.38 A. The following is based table 1 presents the data specifications of the solar panel module used.

Table 1. Solar Panel Specification Data Used [16]

Characteristic	Rating
Max. Power (Pmax)	150 Wp
Optimum Operating Voltage (Vmp)	18.1 V
Optimum Operating Current (Imp)	8.29 A
Open Circuit Voltage (Voc)	22.1 V
Short Circuit Current (Isc)	8.69 A

Battery Storage

The type of battery used in this study, namely Lithium-Ion LFP200AHA 3.2 V [17] was installed in series with four units so that the battery system specification value was obtained, namely 12 V 200 Ah. The following describes the data specifications for the per-cell battery used.

Table 2. Battery Specification Data Used [17]

Characteristic	Rating
Nominal Voltage	3.2 V
Capacity	200 Ah
Operating Voltage (Max – Min)	3.8-2.8 V
Deep Discharge Voltage	2.5 V
Maximal Charge Voltage	4 V
Optimal Discharge Current (0.5 C)	<100 A
Maximal Charge Current (0.5 C)	<100 A

DC-DC Converter

In this study, two types of DC-DC Converters were used, namely DC-DC Buck Converters for charging systems with PV as a source of electrical energy and DC-DC Boost Converters as a discharging system with batteries as a source of electrical energy. Furthermore, the research flowchart for the design of the DC-DC Converter can be seen in figure 2.

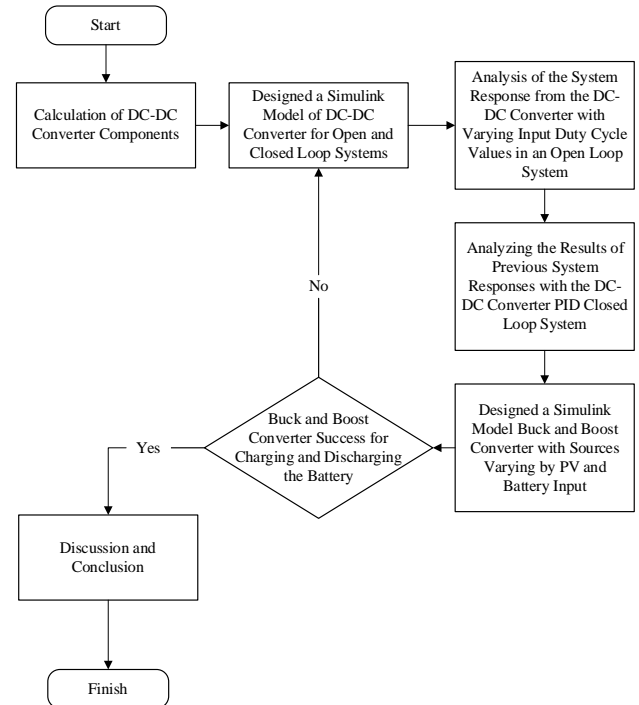


Figure 2. Flowchart for DC-DC Converter Design

Mathematical Calculations for DC-DC Buck Converter Circuit Design as a Power Charging System

As a charging system, the DC-DC Buck Converter in a hybrid PV system is used to lower the source voltage of the PV modules so that it matches the voltage specifications required by the battery. In the following, several mathematical equations [18] are present to obtain the values or specifications of the constituent components of the DC-DC Buck Converter circuit.

- a. Determine the output voltage (Vout)

$$V_{out} = V_{in} \cdot D \tag{1}$$

- b. Determine output current (Iout)

$$I_{out} (max) = \frac{V_{out}}{Rl (min)} \tag{2}$$

$$I_{out} (min) = \frac{V_{out}}{Rl (max)} \tag{3}$$

- c. Determine output power (Pout)

$$P_{out} (max) = V_{out} \cdot I_{out} (max) \tag{4}$$

$$P_{out} (min) = V_{out} \cdot I_{out} (min) \tag{5}$$

- d. Determine the minimum inductor value (Lmin)

$$L_{min} = \frac{Rl \max \left(\frac{1}{\eta} - D_{min} \right)}{2 f s} \tag{6}$$

e. Determine the peak-to-peak current (Δi_l)

$$\Delta i_l \max = \frac{V_{out} (1-D_{min})}{f_s \cdot L} \tag{7}$$

f. Determine voltage stresses ($V_{sm}(\max)$)

$$V_{SM}(\max) = V_{DM}(\max) = V_{Imax} \tag{8}$$

g. Determine current stresses ($I_{sm}(\max)$)

$$I_{SM}(\max) = I_{DM} \max = I_{out} \max + \frac{\Delta i_l}{2} \tag{9}$$

h. Determine the output value of capacitor (C_{out})

$$C_{min} = \frac{D_{max}}{2 f_s \cdot r_c \max} \tag{10}$$

i. Determine power losses (P_{LS})

$$P_{LS} = P_{rDs} + P_{SW} + P_D + P_{rl} + P_{rc} \tag{11}$$

- Power mosfet dissipation (P_{FET})

$$P_{FET} = P_{rDs} + \frac{P_{SW}}{2} \tag{12}$$

- Diode conduction loss (P_D)

$$P_D = P_{VF} + P_{RF} \tag{13}$$

- Inductor loss (P_{rl})

$$P_{rl} = r_l \cdot I_{out}(\max)^2 \tag{14}$$

- Capacitor loss (P_{rc})

$$P_{rc} = \frac{r_c \cdot (\Delta i_l \max)^2}{12} \tag{15}$$

j. Determine the efficiency of the circuit (η)

$$\eta = \frac{P_{out}}{P_{out} + P_{LS}} \times 100\% \tag{16}$$

k. Determine Snubber Converter

- Snubber capacitor (C_{sn})

$$C_{sn} = \frac{I_l \cdot t_f}{2 \cdot v_f} \tag{17}$$

- Snubber resistor (R_{sn})

$$R_{sn} < \frac{t_{on}}{5C} \tag{18}$$

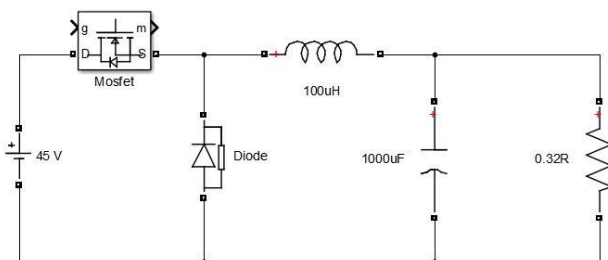


Figure 3. Simulink Model DC-DC Buck Converter

Table 3. DC-DC Buck Converter Component Specifications

Characteristic	Rating
Input Voltage (V_{in})	45 V
Output Voltage (V_{out})	16 V
Duty Cycle (D)	35 %
Maximum Load Resistance (R_{Lmax})	1.6 Ω
Minimum Load Resistance (R_{Lmin})	0.32 Ω
Maximum Output Current (I_{outmax})	50 A
Minimum Output Current (I_{outmin})	10 A
Maximum Output Power (P_{outmax})	800 W
Minimum Output Power (P_{outmin})	160 W
Minimum Inductance (L_{min})	20.64 μ H
Peak-to-Peak current of the inductor (Δi_L)	4.128 A
Semiconductor Voltage Stresses (V_{smmax})	45 V
Semiconductor Current Stresses (I_{smmax})	52.064 A
Minimum Capacitance (C_{out})	183 μ F
Total Power Loss (P_{LS})	224.7 W
Circuit Efficiency (η)	78 %
Snubber Capacitor (C_{sn})	90 nF
Snubber Resistor (R_{sn})	44 m Ω

Mathematical Calculations for DC-DC Boost Converter Circuit Design as a Power Discharge System

As a discharging system, the DC-DC Boost Converter in a PV hybrid system is used to increase the source voltage from the battery to match the voltage specifications required by the inverter. In the following, the inverter data specifications are present, which can be seen in Table 4 [19] to serve as one of the reference values in designing the ideal output value for the dc-dc boost converter. So after that, several mathematical equations are also presented to obtain component values or specifications constituent of the dc-dc boost converter circuit [18].

Table 4. Specifications of the GTI-D1000B Inverter [19]

Characteristic	Rating
Output Power	950 W
Optimum Operating Voltage (V_{mp})	35-39 V
Open-Circuit Voltage (V_{oc})	42-45 V
MPPT Voltage Range	30-40 V
AC Voltage Range	190~260 V

a. Determine the output voltage (V_{out})

$$V_{out} = \frac{V_{in}}{1-D} \tag{19}$$

b. Determine output current (I_{out})

$$I_{out}(\max) = \frac{V_{out}}{R_l(\min)} \tag{20}$$

$$I_{out}(\min) = \frac{V_{out}}{R_l(\max)} \tag{21}$$

c. Determine output power (P_{out})

$$P_{out}(\max) = V_{out} \cdot I_{out}(\max) \tag{22}$$

$$P_{out}(\min) = V_{out} \cdot I_{out}(\min) \tag{23}$$

d. Determine the minimum inductor value (L_{min})

$$L_{min} = \frac{Rl \max \cdot D (1-D)^2}{2 \cdot fs} \tag{24}$$

e. Determine the peak-to-peak current (Δi_l)

$$\Delta i_l = \frac{V_{out} \cdot D (1-D)}{fs \cdot L} \tag{25}$$

f. Determine voltage stresses (V_{sm(max)})

$$V_{SM(max)} = V_{DM(max)} = V_{OUT(max)} \tag{26}$$

g. Determine current stresses (I_{sm(max)})

$$I_{SM \max} = I_{DM \max} = I_{imax} + \frac{\Delta i_l \max}{2} \tag{27}$$

h. Determine the output value of capacitor (C_{out})

$$C_{min} = \frac{Dmax \cdot V_{out}}{fs \cdot Rlmin \cdot V_{cpp}} \tag{28}$$

i. Determine power losses (P_{LS})

$$P_{LS} = P_{rDs} + P_{SW} + P_D + P_{rl} + P_{rc} \tag{29}$$

- Power mosfet dissipation (P_{FET})

$$P_{FET} = P_{rDs} + \frac{P_{SW}}{2} \tag{30}$$

- Diode conduction loss (P_D)

$$P_D = P_{VF} + P_{RF} \tag{31}$$

- Inductor loss (P_{rl})

$$P_{rl} = rl \cdot I_{rms}^2 \tag{32}$$

- Capacitor loss (P_{rc})

$$P_{rc} = rc \cdot I_{C_{rms}}^2 \tag{33}$$

j. Determine the efficiency of the circuit (η)

$$\eta = \frac{P_{out}}{P_{out} + P_{LS}} \times 100\% \tag{34}$$

k. Determine Snubber Converter

- Snubber capacitor (C_{sn})

$$C_{sn} = \frac{Il \cdot t_f}{2 \cdot v_f} \tag{35}$$

- Snubber Resistor (R_{sn})

$$R_{sn} < \frac{t_{on}}{5C} \tag{36}$$

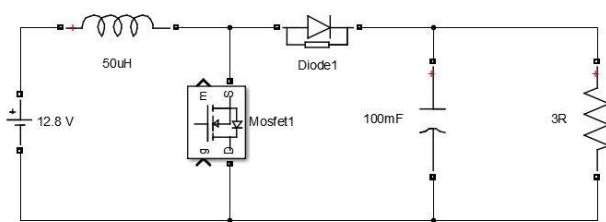


Figure 4. Simulink Model DC-DC Boost Converter

Table 5. DC-DC Boost DC Converter Component Specifications

Characteristic	Rating
Input Voltage (V _{in})	12.8 V
Output Voltage (V _{out})	45 V
Duty Cycle (D)	71 %
Maximum Load Resistance (R _{Lmax})	5 Ω
Minimum Load Resistance (R _{Lmin})	3 Ω
Maximum Output Current (I _{outmax})	15 A
Minimum Output Current (I _{outmin})	10 A
Maximum Output Power (P _{outmax})	675 W
Minimum Output Power (P _{outmin})	450 W
Minimum Inductance (L _{min})	7.66 μH
Peak-to-Peak current of the inductor (Δi _L)	7.41 A
Semiconductor Voltage Stresses (V _{smmax})	45 V
Semiconductor Current Stresses (I _{smmax})	18.70 A
Minimum Capacitance (C _{out})	1.89 mF
Total Power Loss (PLs)	158.53 W
Circuit Efficiency (η)	80 %
Snubber Capacitor (C _{sn})	46.57 nF
Snubber Resistor (R _{sn})	107 mΩ

Full-Bridge Inverter Single Phase (DC-AC)

The design of the inverter in this study is limited to showing that the output value produced by the Simulink Model dc-dc boost converter with a battery as the energy source can indeed be used to supply inverters with similar specifications as attached in Table 4, which can also be used as a reference in determining the output value of the boost converter when designing.

In addition, with the same inverter input value range, this study shows that the PV Array can also be used as a hybrid PV energy source, as shown in Figure 1, which can also be used to supply inverters directly to meet load demand.

Based on Figure 5, it can be seen that to carry out the unipolar switching method on a full-bridge inverter, two sinusoidal signals with a frequency of 50 Hz are required by a sine wave component with a phase angle difference of 180°, which will then be modulated by a carrier signal in the form of a triangle wave with a frequency of 1000 Hz by sawtooth generator component, after which the modulated signal will be forwarded to the semiconductor components S1, S2, S3, S4 (IGBT) which are arranged in the form of a full bridge inverter. Figure 6 shows Simulink model of DC-DC buck and boost converter in hybrid PV systems.

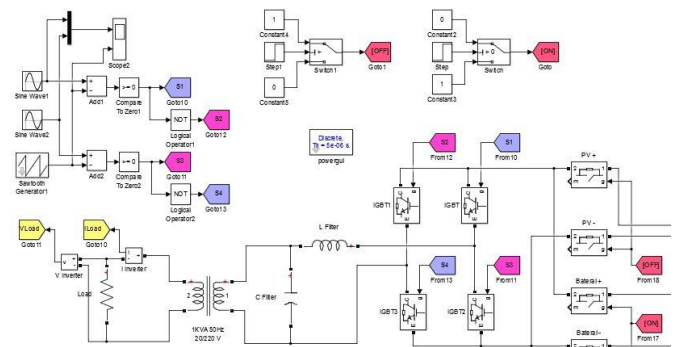


Figure 5. Full-Bridge Single Phase Inverter with Unipolar SPWM Switching

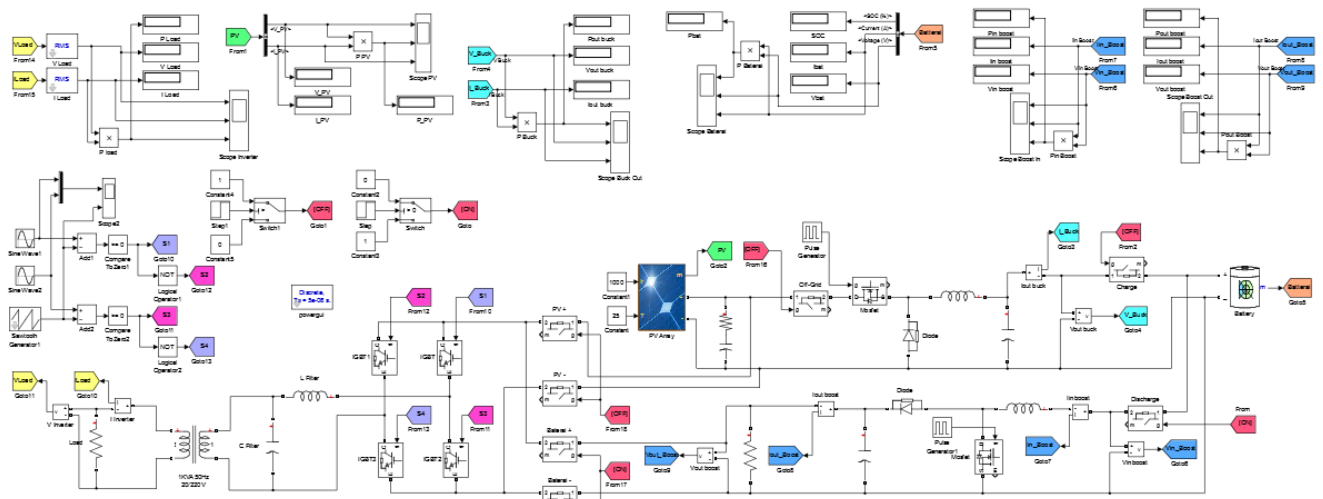


Figure 6. Simulink Model DC-DC Buck and Boost Converter in Hybrid PV Systems

RESULTS AND DISCUSSION

Analysis of DC-DC Converter System Response With a Fixed Source

After testing the DC-DC Converter with a fixed source, as shown in Figure 3 and 4. Then the result is obtained that by giving a switching frequency value of 25 kHz by the IC components used, as well as by varying the duty cycle value in the system, then the results will be obtained which is following the theory, where the smaller the duty cycle value given to the buck converter, the output voltage value to the input voltage will decrease, namely

from 45 V to 33.9 – 1.46 V. Meanwhile in the boost converter, the greater the value is given duty cycle, the value of the output voltage to the input voltage will also increase, from 12.8 V to 16.90 – 33.49 V. Furthermore, Tables 6 and 7 show a comparison of the response results of the transition system with and without PID on the DC-DC Converter, as shown in Figures 7-10.

Furthermore, based on the test results summarized in Tables 6 and 7, it can be concluded that a closed loop system equipped with a PID controller on the buck and boost converter, as seen in Figures 8 and 10, can function to reduce the overshoot value in the transition system response.

Table 6. Response Data for Open and Closed Loop DC-DC Buck Converter Systems with a Duty Cycle Value of 35%

Parameter	Buck Converter Open Loop (Without PID Controller)		Buck Converter Close Loop (With PID Controller)	
	Vout	Iout	Vout	Iout
Amplitude	13,66V	42,70A	15,84V	49,52A
High	13,74V	42,95A	15,92V	49,77A
Low	78,6mV	245,9mA	80,1mV	250,5mA
Rise Time	502,7µs	502,7µs	3,07ms	3,07ms
Settling Time	2,03ms	2,03ms	8,17ms	8,17ms
Preshoot	0,57%	0,57%	0,50%	0,50%
Overshoot	14,36%	14,36%	0,24%	0,24%
UnderShoot	2,49%	2,49%	3%	3%
Max	15,71V	49,09A	16,01V	50,03A
Min	144µV	449,9µA	144µV	449,9µA
Peak to Peak	15,71V	49,10A	16,01V	50,02A
Mean	13,69V	42,79A	15,97V	49,92A
Median	13,70V	42,80A	15,99V	49,99A
RMS	13,70V	42,80A	15,98V	49,93A

Table 7. Response Data for DC-DC Boost Converter Open and Closed Loop Systems with a 70% Duty Cycle

Parameter	Boost Converter Open Loop (Without PID Controller)		Boost Converter Close Loop (With PID Controller)	
	Vout	Iout	Vout	Iout
Amplitude	32,86V	10,95A	31,35V	10,45A
High	33,03V	11,01A	31,51V	10,50A
Low	166mV	55,3mV	158,3mV	52,7mA
Rise Time	83,29ms	83,29ms	72,90ms	72,90ms
Settling Time	-	-	127ms	127ms
Preshoot	0,50%	0,50%	-	-
Overshoot	0,47%	0,47%	0%	0%
UnderShoot	2,00%	2,00%	-	-
Max	33,20V	11,06A	31,66V	10,55A
Min	- 6,2μ V	-2,0μ A	-7,0μ V	-2,3μ A
Peak to Peak	33,20V	11,06A	31,66V	10,55A
Mean	31,48V	0,50A	29,31V	9,77A
Median	32,97V	0,47A	30,75V	10,25A
RMS	31,66V	2A	29,48V	9,82A

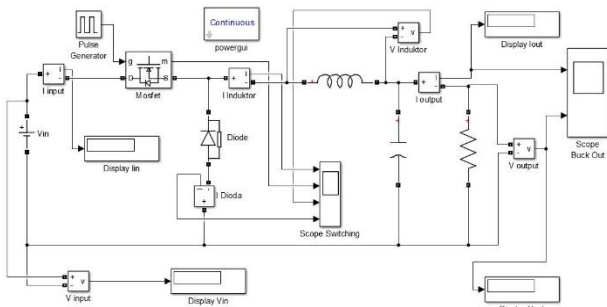


Figure 7. Open Loop System Buck Converter Without PID

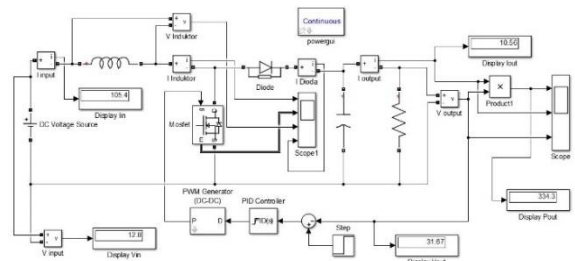


Figure 10. Closed Loop System Boost Converter With PID

Analysis of DC-DC Converter System Responses With Varying Sources

Buck Converter As a Charging Systems (DC-DC)

Based on the PV 600 Wp test connected to the DC-DC Buck and Boost Converter for the LFP200AHA lithium-ion battery charging process, as in figure 11. Then the results of the system response are obtained as attached in Figure 12, namely in the form of a change in the output current and voltage values on the battery and buck converter side when the solar irradiation (IR) value received by the PV array changes from 0 W/m² - 1000 W/m², as is the case in Table 8. Furthermore, based on Figure 12, especially in the SOC signal section it can also be seen that the designed system has been successful and can work properly for the battery charging process, where this can be indicated by changes in the SOC signal which tends to increase in the system as the change in solar irradiation value, apart from that with variations in irradiation received by the PV in the system. Of course, can also affect the battery charging time.

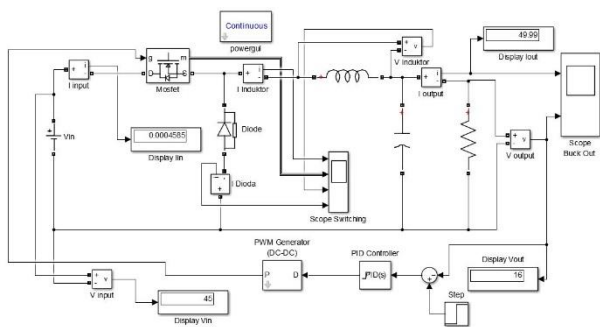


Figure 8. Closed Loop System Buck Converter With PID

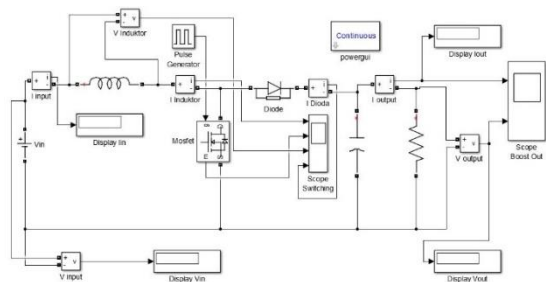


Figure 9. Open Loop System Boost Converter without PID

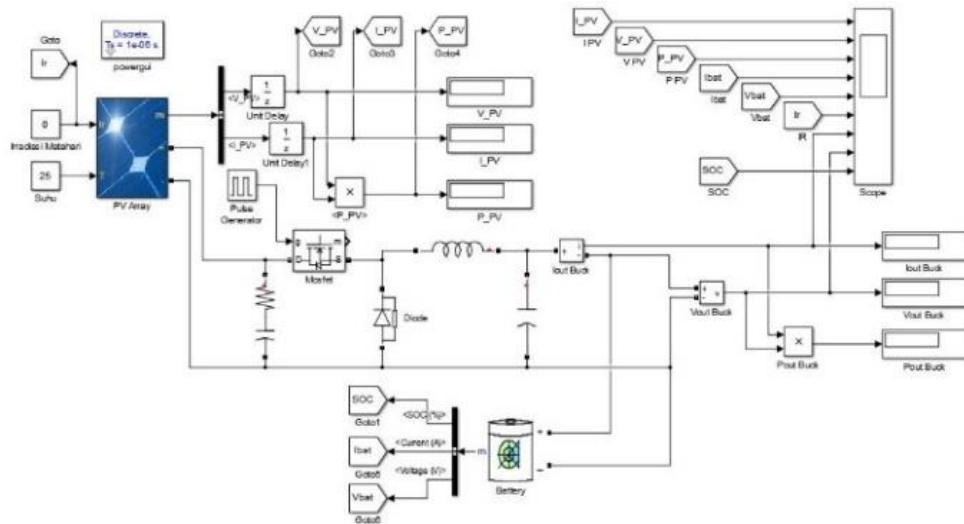


Figure 11. Simulink Model of 600 Wp Solar Panel Connected DC-DC Buck Converter and Lithium-Ion Battery LFP200AHA

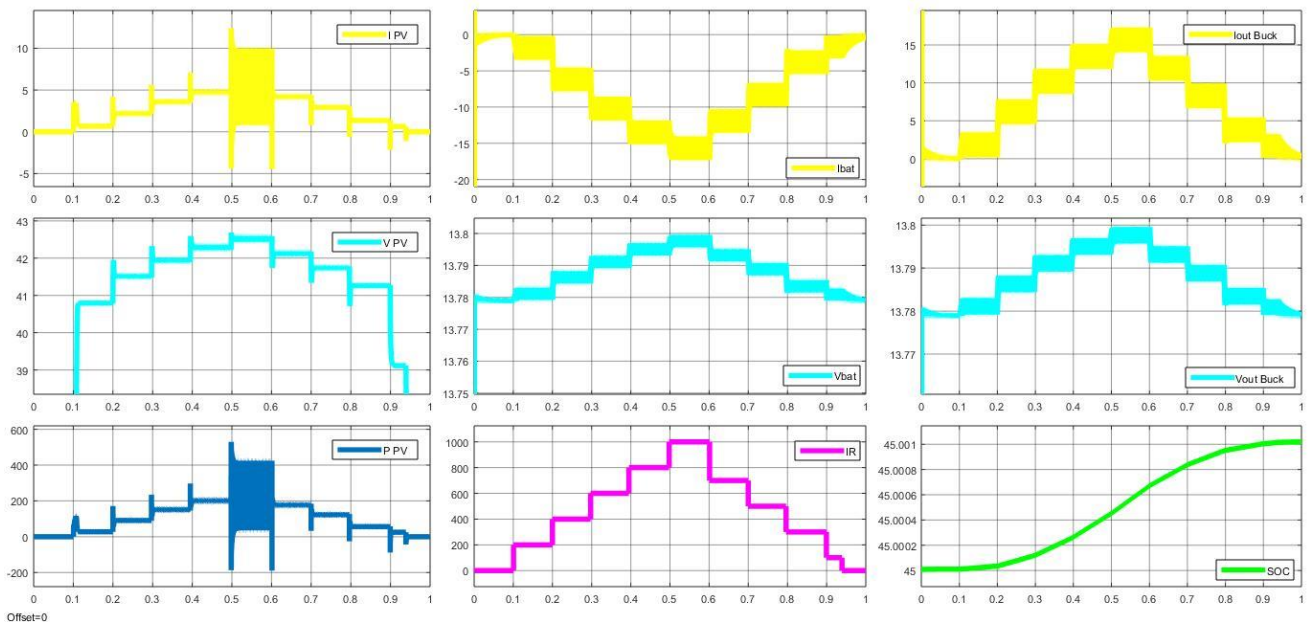


Figure 12. The plot of Output Current and Voltage Curves on the Sides of Solar Panels, Buck Converters, and Batteries with Various Irradiations for the Charging Process

Table 8. Result Data for PV 600 Wp Connected DC-DC Buck Converter for Charging LFP200AHA 12V 200Ah Battery with a Duty Cycle Value of 35%

Solar irradiation (W/m ²)	Solar Panel			Buck Converter			Battery		
	Pout (W)	Iout (A)	Vout (V)	Pout (W)	Iout (A)	Vout (V)	Pbat (W)	Ibat (A)	Vbat (V)
0	-121,28μ	-6,90μ	17,56	-34,49m	-2,50m	13,77	34,49m	2,50m	13,77
200	27,38	667,1m	40,80	4,46	323,8m	13,77	-4,46	-323,8m	13,77
400	89,05	2,14	41,53	62,57	4,54	13,78	-62,57	-4,54	17,78
600	147,40	3,51	41,98	120,19	8,71	13,78	-120,19	-8,71	13,78
800	195,07	4,60	42,34	165,50	11,99	13,79	-165,50	-11,99	13,79
1000	404,02	10,01	42,57	231,79	16,71	13,79	-231,79	-16,71	13,79

DC-DC Boost Converter As a Discharge Systems (DC-DC)

Based on testing, the LFP200AHA lithium-ion battery connects to the DC-DC Boost Converter for the battery discharge process, as in figure 13. Then the results of the system response are obtained, as attached in Figure 14. Namely, the system can work for the battery discharge process, where this is indicated by

changes in the SOC signal, which tends to decrease in the system over time, and based on the results of the battery discharge plot used in Figure 9, shows that setting the size of the output current to supply the load requirements also affects the battery lifetime. Therefore, setting the correct duty cycle value, as shown in Table 9, also has a major effect on the system.

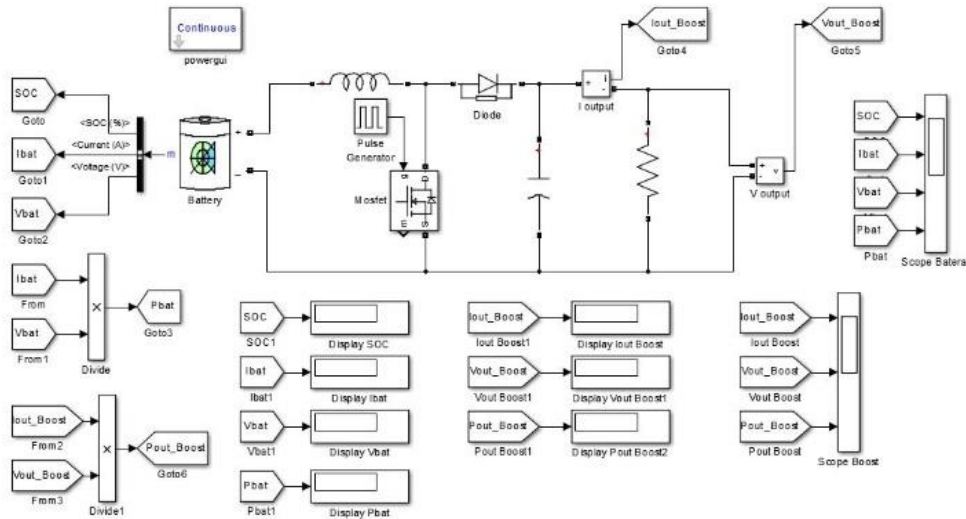


Figure 13. Simulink Model of Lithium-ion Battery LFP200AHA Connected DC-DC Boost Converter

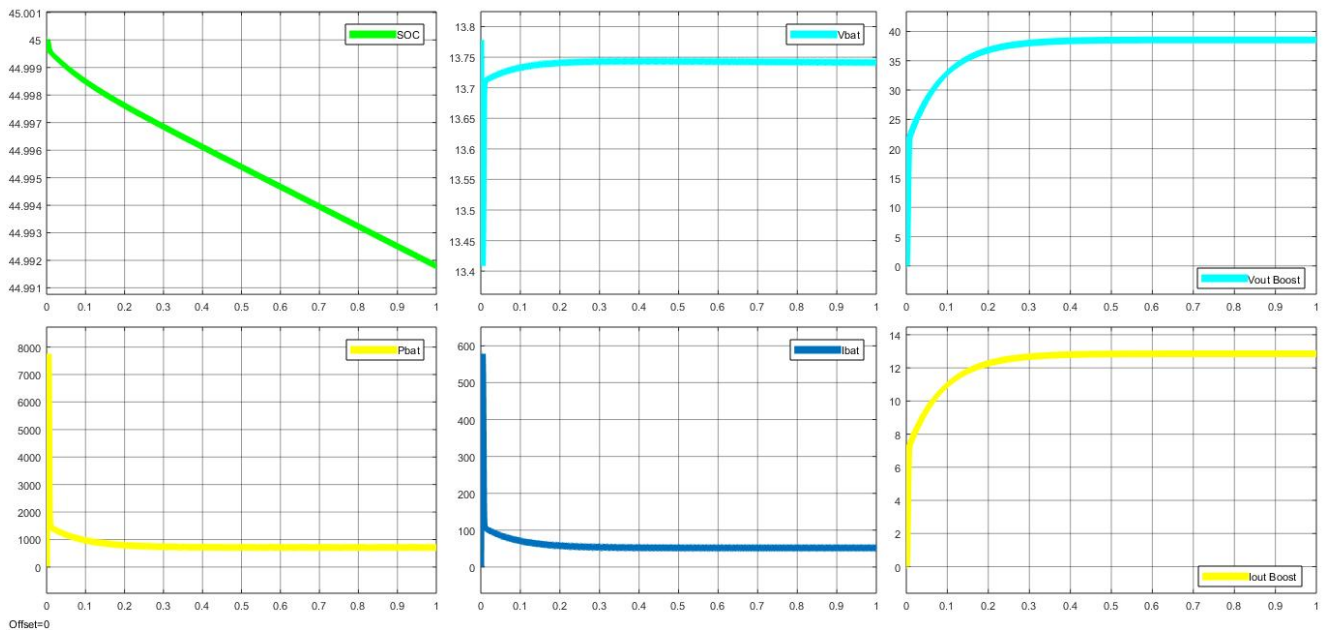


Figure 14. The plot of the Output Current and Voltage Curves on the Battery Side and the Boost Converter for the Discharging Process

Table 9. Result Data for LFP200AHA Lithium-Ion Battery Connected to DC-DC Boost Converter

Duty Cycle (%)	Battery			Boost Converter		
	Battery Voltage (V)	Battery Current (A)	Battery Power (W)	Output Voltage (V)	Output Current (A)	Output Power (W)
10	13,767	15,963	215,218	17,475	5,825	108,078
20	13,767	16,916	228,305	18,507	6,169	118,606
30	13,763	21,566	291,383	19,322	6,441	126,170
40	13,760	24,029	325,520	21,417	7,139	153,092
50	13,755	31,213	423,526	24,951	8,317	207,762
60	13,748	39,055	531,686	29,527	9,842	291,510
70	13,737	53,341	728,546	34,845	11,615	408,048
80	13,716	79,278	1085	38,558	12,853	504,523
90	13,687	119,493	1634	31,238	10,413	331,509

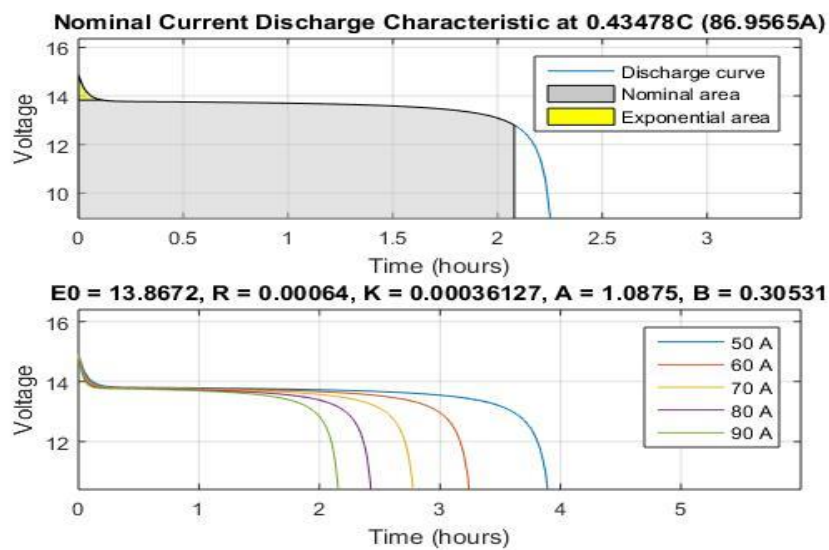


Figure 15. The plot of Discharge Characteristics of the LFP200AH Lithium-Ion Battery

Analysis of PV 600 Wp and Lithium-Ion Battery 200 Ah as the main source in PV Hybrid systems (DC-AC)

PV as an Energy Source (DC-AC)

Based on the Simulink testing of the hybrid PV system model in Figure 6, which further obtained the system plot results in Figure 16 below, it can be seen that the 600 Wp solar panel with measured PV voltage and current of 33.34V and 17.21A, when connected to the inverter, can generate ac electricity on the load side with RMS voltage and current values of 170.44V and 900.97mA.

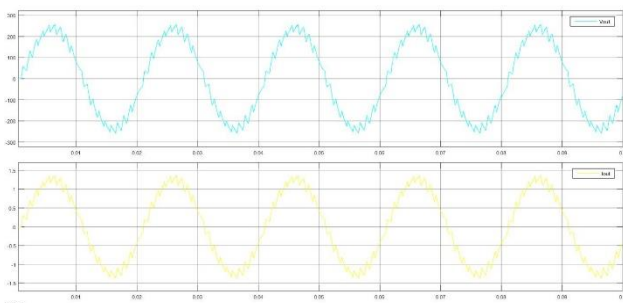


Figure 16. Inverter Output Signals When Supplied by PV

Battery As Energy Source (DC-AC)

Furthermore, based on the Simulink testing of the Hybrid PV system model in Figure 6, which further obtained the system plot results in Figure 17 below, it can be seen that the 12V 200Ah lithium-ion battery is passed through the dc-dc boost converter first or with the boost converter output voltage and current being measured, which is equal to 34.84V and 11.61A, then when connected to the inverter can generate ac electricity on the load side with RMS voltage and current values of 148.58V and 785.40mA

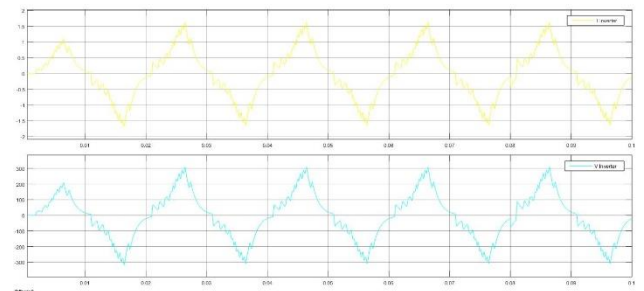


Figure 17. Inverter Output Signal When Supplied by a Battery

CONCLUSIONS

The designed hybrid PV system successfully charges batteries during periods of excess PV generation through a buck converter, stepping down the 600 Wp PV voltage from $\pm 44.2\text{V}$ to 13.77–13.79V by adjusting the 35% duty cycle. For discharging, the boost converter increases the 12.8V lithium-ion battery voltage to 34.84V using a 70% duty cycle, providing power during high demand nighttime hours.

Recommendations for further work include adding constant current (CC) or constant current, constant voltage (CC/CV) control to the buck converter to prevent battery overcharge and optimize charging current. Similarly, constant voltage (CV) or CC/CV control would allow the boost converter to produce larger, more constant output voltages as needed by the inverter specifications. Finally, incorporating a maximum power point tracking (MPPT) system would allow the PV system and converters to approach maximum power generation capacity.

REFERENCES

- [1] U. Simanjuntak, "IETO 2023: Antisipasi Krisis Energi dengan Pemanfaatan Energi Terbarukan." Accessed: Jun. 03, 2023. [Online]. Available: <https://iesr.or.id/ieto-2023-antisipasi-krisis-energi-dengan-pemanfaatan-energi-terbarukan>
- [2] K. B. Pratama, "Energi Transisi sebagai Alternatif Penekan Laju Pemanasan Global." Accessed: Jun. 03, 2023. [Online]. Available: <https://www.its.ac.id/news/2022/12/13/energi-transisi-sebagai-alternatif-penekan-laju-pemanasan-global/>
- [3] A. Setyarto, "Langkah Menuju Transisi Energi." Accessed: Jun. 03, 2023. [Online]. Available: <https://ppsdmaparatur.esdm.go.id/berita/langkah-menuju-transisi-energi>
- [4] EBTKE, "Upaya Pemanfaatan Energi Terbarukan, Wamen Arcandra: Kuncinya Data." Accessed: Feb. 27, 2023. [Online]. Available: <https://ebtke.esdm.go.id/post/2018/04/09/1930/upaya.pemanfaatan.energi.terbaru>
- [5] R. Ridwan, W. Ramadhan, A. Kurniawan, W. Lestari, and D. Setiawan, "Pemanfaatan Sinar Matahari Sebagai Energi Alternatif Untuk Kebutuhan Energi Listrik," *SENKIM: Seminar Nasional Karya Ilmiah Multidisiplin*, vol. 1, no. 1, pp. 168–176, 2021.
- [6] T. Alamsyah, A. Hiendro, and Z. Abidin, "Analisis Potensi Energi Matahari Sebagai Pembangkit Listrik Tenaga Surya Menggunakan Panel Monocrystalline dan Polycrystalline Di Kota Pontianak dan Sekitarnya," *Journal of Electrical Engineering, Energy, and Information Technology*, vol. 9, no. 2, 2021.
- [7] I. G. N. N. Santhiarsa and I. G. B. W. Kusuma, "Kajian Energi Surya Untuk Pembangkit Tenaga Listrik," *Majalah Ilmiah Teknologi Elektro*, vol. 4, no. 1, pp. 29–33, 2005.
- [8] E. Prasetyono, W. Ashary, A. Tjahjono, and N. A. Windarko, "Studi Komparasi Fungsi Keanggotaan Fuzzy sebagai Kontroler Bidirectional DC-DC Converter pada Sistem Penyimpan Energi," *Jurnal Nasional Teknik Elektro*, vol. 4, no. 2, p. 172, Sep. 2015, doi: 10.25077/jnte.v4n2.161.2015.
- [9] G. de Oliveira e Silva and P. Hendrick, "Photovoltaic self-sufficiency of Belgian households using lithium-ion batteries, and its impact on the grid," *Appl Energy*, vol. 195, pp. 786–799, Jun. 2017, doi: 10.1016/j.apenergy.2017.03.112.
- [10] A. Smets, K. Jäger, O. Isabella, R. van Swaaij, and M. Zeman, *Solar Energy: The physics and engineering of photovoltaic conversion, technologies and systems*. Cambridge: UIT Cambridge Limited, 2016.
- [11] F. K. Jean-Rostand, M. M. Mustapha, I. Adabara, and A. S. Hassan, "Design of an Automatic Transfer Switch for Households Solar PV System," *European Journal of Advances in Engineering and Technology*, vol. 6, no. 2, pp. 54–65, 2019.
- [12] M. Ali, *Aplikasi Elektronika Daya pada Sistem Tenaga Listrik*. Yogyakarta: UNY Press, 2018.
- [13] N. Kshatri, S. Kumar, and R. Mishra, "An Innovate on Hybrid Power Generation on DC–DC Buck Converter with MPPT Systems," *Turkish Journal of Computer and Mathematics Education (TURCOMAT)*, vol. 11, no. 3, pp. 1741–1758, 2021.
- [14] K. A. Ogudo and P. Umenne, "Design of a PV Based Power Supply with a NonInverting Buck-Boost Converter," in *2019 IEEE PES/IAS PowerAfrica*, IEEE, Aug. 2019, pp. 545–549. doi: 10.1109/PowerAfrica.2019.8928656.
- [15] I. Jagadeesh and V. Indragandhi, "Comparative Study of DC-DC Converters for Solar PV with Microgrid Applications," *Energies (Basel)*, vol. 15, no. 20, p. 7569, Oct. 2022, doi: 10.3390/en15207569.
- [16] SOLANA, "Mono Crystalline Solar Panel," solana.co.id. Accessed: Jun. 11, 2023. [Online]. Available: <https://solana.co.id/monocrystalline/>
- [17] GWL, "Winston LFP200AHA Cell," [gwl.eu](https://files.gwl.eu/inc/_doc/attach/StoItem/1124/ThunderSky-Winston-LIFEPO4-200Ah-WIDE-Datasheet.pdf). Accessed: Jun. 11, 2023. [Online]. Available: https://files.gwl.eu/inc/_doc/attach/StoItem/1124/ThunderSky-Winston-LIFEPO4-200Ah-WIDE-Datasheet.pdf
- [18] M. K. Kazimierczuk, *Pulse-width modulated DC-DC power converters*, Kedua. Chichester: John Wiley & Sons, Ltd, 2016. doi: 10.1002/9781119009597.
- [19] SUOER, "GTI-D1000B," [chinasuoer.com](http://www.chinasuoer.com). Accessed: Jun. 15, 2023. [Online]. Available: <http://www.chinasuoer.com/grid-tie-inverter/gti-d1000b.html>